Solar Energy Materials and Solar Cells 168 (2017) 234–240

Contents lists available at ScienceDirect

Solar Energy Materials and Solar Cells

journal homepage: www.elsevier.com/locate/solmat

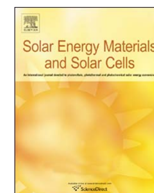

Radiation hardness of AlGaAs *n-i-p* solar cells with higher bandgap intrinsic region

A.W. Walker*, S. Heckelmann, T. Tibbits, D. Lackner, A.W. Bett, F. Dimroth

Fraunhofer Institute for Solar Energy Systems ISE, Heidenhofstraße 2, 79110 Freiburg, Germany

ARTICLE INFO

Keywords:
AlGaAs
n-i-p solar cell
Radiation hardness
End-of-life
Diffusion length
Device modeling

ABSTRACT

The radiation hardness of AlGaAs single-junction solar cells is investigated for various *n-i-p* solar cell designs. The material composition in both the *n-p* regions is varied between 3.5% and 16% Al-content, whereas the intrinsic region has a higher Al-content between 3.5% and 23%. The beginning-of-life and end-of-life quantum efficiency and current – voltage characteristics are discussed to establish trends as a function of material bandgap. It is found that, increasing the Al-content of AlGaAs tends to increase the radiation hardness of the solar cells up to an efficiency remaining factor of 85%. This enhancement mostly originates from an improved open circuit voltage remaining factor that is caused by a deterioration of the beginning-of-life performance as the Al-content increases. However, a degradation in photocurrent is observed for increasing Al content in the intrinsic region, which is partially due to minority carrier potential barriers at the base/intrinsic heterointerface. In general, increasing the bandgap of the intrinsic region improves radiation hardness, but the formation of potential barriers for minority carriers must be avoided. The diffusion lengths and damage coefficients are also extracted by modeling the quantum efficiency.

1. Introduction

The radiation hardness of III-V semiconductor materials is crucial to the long lasting operation of photovoltaic devices in severe conditions such as in low and high altitude satellite orbits. High-energy particles bombarding devices create displacement damage in the crystal structure, which results in the creation of defects within the active semiconductor materials that act as efficient non-radiative recombination centers and influence carrier removal rates. Typically, concepts such as non-ionizing energy loss [1,2] and the corresponding displacement damage dose [3–5] have been discussed in the literature to rate how different semiconductors degrade under irradiation. These parameters can also be used to empirically predict how cells will perform in their end-of-life (EOL). The degradation of these devices can also be gauged by modeling the external quantum efficiency or using electron beam-induced current, both of which extract the damage coefficients for the diffusion length as a function of irradiation [6–9]. The use of deep-level transient spectroscopy also gives insight into the concentration and types of traps created due to irradiation [10–14]. Multiple methods thus exist to study the degradation mechanisms in solar cells, all of which eventually refer to the efficiency remaining factors.

In most radiation hardness studies, the cell designs are typically *p-n* homojunctions, as these are the simplest and most common structures to investigate. Heterojunctions are not commonly reported on, primarily because the analysis becomes obfuscated, i.e. how much each material contributes to the overall degradation. Yet heterojunctions have previously been used to boost beginning-of-life (BOL) device performance via an enhanced open circuit voltage, most notably in GaAs/AlGaAs systems [15]. Furthermore, AlGaAs can be expected to have a higher resistance to radiation damage due to its higher bandgap, since it exponentially reduces the intrinsic carrier concentration, thereby limiting the Shockley-Read-Hall (SRH) contribution to the dark current, which is the dominant source of dark current in irradiated solar cells. For an AlGaAs homojunction, the stronger absorption coefficient close to its bandgap for increasing Al-content (within its direct bandgap regime) [16,17] leads to thinner cell requirements and reduces the impact of diffusion length degradation in EOL material. This enhances the radiation hardness even if the minority carrier damage coefficients for AlGaAs are nearly the same as for GaAs [8]. The possibility of improved radiation hardness using heterostructures consisting of higher bandgap AlGaAs materials thus merits further study and analysis, although only within the Al content range where DX centers are not relevant [18-21].

This paper reports on *n-i-p* $Al_xGa_{1-x}As/Al_yGa_{1-y}As/Al_xGa_{1-x}As$ solar cells of varying Al molar fractions y in the intrinsic region compared to the *n-p* emitter-base layers. Section 2 describes the samples

* Corresponding author. Present address: National Research Council of Canada, 1200 Montreal Road, Ottawa, Ontario, Canada.
E-mail address: alexandre.walker@nrc-cnrc.gc.ca (A.W. Walker).

http://dx.doi.org/10.1016/j.solmat.2017.04.034
Received 6 February 2017; Accepted 19 April 2017
Available online 19 May 2017
0927-0248/ © 2017 Elsevier B.V. All rights reserved.

MgF$_2$/Ta$_2$O$_5$ anti-reflection coating		
30 nm	n-GaInP:Si window	2.0E18 cm^{-3}
120 nm	n-Al$_x$Ga$_{1-x}$As:Te emitter	1.0E18 cm^{-3}
500 nm	*i*-Al$_y$Ga$_{1-y}$As	1.0E16 cm^{-3}
2000 nm	p-Al$_x$Ga$_{1-x}$As:C base	9.0E16 cm^{-3}
125 nm	p-Al$_{0.3}$Ga$_{0.7}$As:C barrier	5.0E18 cm^{-3}
500 nm	p-GaAs:Zn buffer	1.0E18 cm^{-3}
450 µm	p-GaAs:Zn substrate	1.0E18 cm^{-3}

Fig. 1. Structural details of the AlGaAs single-junction solar cells grown on a GaAs substrate. The molar fraction x of Al$_x$Ga$_{1-x}$As represents the composition of the emitter and base, and the molar fraction y represents the composition of the intrinsic region, which is intentionally p-doped to 1.0E16 cm^{-3}. Layer thicknesses and doping concentrations remain fixed in this study.

of interest to this study. Section 3 then discusses the results, first in terms of the BOL performance in Section 3.1. End-of-life performances are then discussed in Section 3.2, along with the remaining factors as a function of the intrinsic region's bandgap. Finally, modeling these devices allows for the extraction of the transport parameters (namely the diffusion length) for both BOL and EOL, thus resulting in the diffusion length damage coefficient, which is discussed in Section 3.3. The conclusions of this study are given in Section 4.

2. Samples and designs

2.1. Common sample structure

The structures of interest to this study involve *n-i-p* solar cells grown upright on GaAs wafers with a (100) orientation and a 6° offcut toward the (111) plane. All samples are grown using metal-organic vapor phase epitaxy in an AIXTRON 2800-G4 reactor configured for 8 × 4″ wafer growth. Fig. 1 illustrates the common structure configuration consisting of an *n*-GaInP:Si window layer, an *n*-Al$_x$Ga$_{1-x}$As:Te emitter, a 500 nm i-Al$_y$Ga$_{1-y}$As region followed by 2000 nm of *p*-Al$_x$Ga$_{1-x}$As:C base. Finally, a 125 nm thick *p*-Al$_{0.3}$Ga$_{0.7}$As:C back surface field is employed on the rear-side. Standard photolithography, mesa etching and metal evaporation were used for solar cell fabrication, resulting in 2 × 2 cm^2 cells. An anti-reflection coating composed of MgF$_2$/Ta$_2$O$_5$ was deposited to minimize incident reflectivity across the wavelength range of absorption in the active region.

Table 1
Al-content of all samples explored in terms of emitter, intrinsic region and base layers.

Sample	Emitter Al-content,Al-content, x [%]	Intrinsic region Al-content,Al-content, y [%]	Base Al-content,Al-content, x [%]
*C2383**	3.5	3.5	3.5
C2389	3.5	7.5	3.5
C2394	3.5	10	3.5
C2395	3.5	13.5	3.5
C2396	10	16.5	10
C2397	16.5	23	16.5

* reference

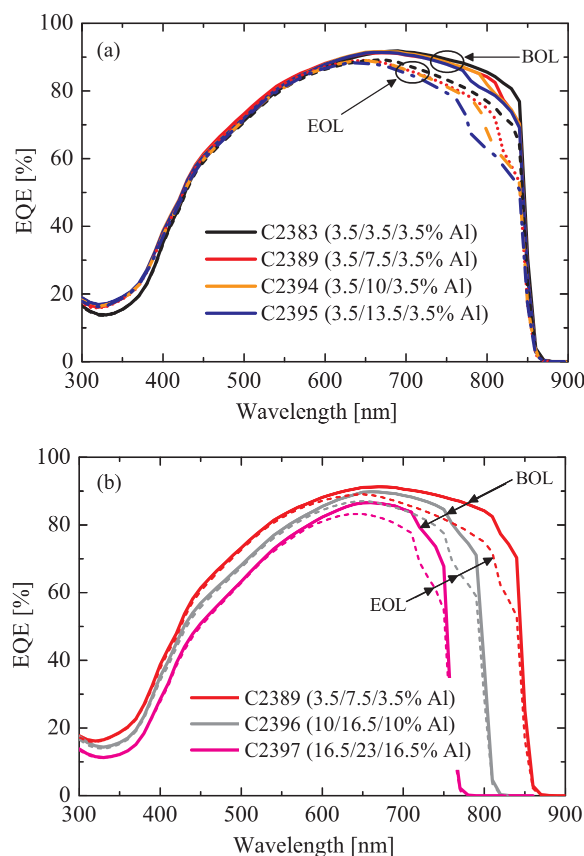

Fig. 2. Measured external quantum efficiency of samples a) C2383, C2389, C2394 and C2395, and b) C2389 compared to C2396 and C2397, for both BOL and EOL. The Al-contents are marked for each sample for the legend for the *n/i/p* Al-contents respectively.

2.2. Sample designs

All samples studied here are derivatives of the previous structure. The principal variations include: 1) the Al content of the emitter and base (x), and 2) the Al content of the intrinsic region (y). Table 1 illustrates the principal design variations and the corresponding sample number, which will be used to refer to the samples hereafter. Note that the Al$_{0.035}$Ga$_{0.965}$As homojunction sample C2383 will be referred to as the reference sample.

3. Results

3.1. Beginning of life performance

3.1.1. External quantum efficiency

The external quantum efficiency (EQE) of samples C2383, C2389, C2394 and C2395 are outlined in Fig. 2a before irradiation, including a comparison to EOL which is discussed in the next section. These samples are chosen to demonstrate the influence of solely increasing the intrinsic region's Al-content on the EQE from 3.5% to 7.5% to 10% and to 13.5% respectively while maintaining 3.5% Al-content in the emitter and base layers. A number of important observations can be made about these designs. First and foremost, the longest wavelength component of the EQE is reduced for increasing Al-content in the intrinsic region, simply because there is 500 nm of Al$_y$Ga$_{1-y}$As with higher Al-content and lower absorption introduced in each sample. The absorption range of the intrinsic region (and thus its bandgap) is clearly seen based on this drop in EQE prior to the band-edge of the base material. The remaining portions of the EQE are very similar, with the exception of the shortest wavelength region between 300 and 400 nm whereby variations are within the margin of error for layer thicknesses

Download English Version:

https://daneshyari.com/en/article/4758802

Download Persian Version:

https://daneshyari.com/article/4758802

Daneshyari.com